k–ω RANS channel flow solver verification

Date: 2/25/2026

Name: Aiden Wang

Couse: ME 5351 (Computational Heat Transfer)

1. Introduction & Objective

Introduction
Credible CFD requires verification. Fully developed turbulent channel flow is a compact, well understood test case for both: it is sensitive to near-wall modeling, turbulence closure coefficients, and grid/time-step choices, while offering clear validation targets such as friction factor and mean velocity profiles. Here, a wall-resolved k–ω RANS model is used to simulate channel flow driven by a constant pressure gradient forcing, enabling rapid convergence to a fully developed state without an entrance region.

Objectives:
The primary goals of this analysis are to:

1. Drive the simulation to a target Reynolds number of Re ≈ 10000 by balancing the applied steam wise pressure gradient (DPDX) against the wall friction

2. Conduct a grid dependency study to evaluate the sensitivity of the k–ω model 1st-order spatial discretization scheme to mesh resolution. This include analyzing the y^+ parameter and addressing the how CFL effect the stability.

3. Calculate the final steady state Darcy friction factor, and compare against the Moody chart for a smooth pipe.

2. Methodology

Turbulence Model Implementation
To close the Reynolds-averaged momentum equations, a standard two-equation k–ω eddy-viscosity model was implemented. The k–ω model is implemented by solving two additional scalar equations for k and ω at each pseudo-time step. After updating k and ω, the eddy viscosity is computed as $\nu_t = k/\omega$, and the solver uses the effective viscosity $\nu_{\text{eff}} = \nu + \nu_t$ in the viscous and diffusive terms of the mean-momentum discretization.

All k–ω coefficients were set to the lecture-provided baseline values

- $\alpha = 5/9$

- $\beta = 3/40$

- $\beta^* = 0.09$

- $\sigma_k = 0.5, \sigma_\omega = 0.5$

To prevent numerical breakdown from division by very small turbulence variables during startup and near-wall updates, lower bounds were enforced:

- $k \geq 10^{-15}$

- $\omega \geq 10^{-6}$

The eddy viscosity is computed using the implemented relation

$$\nu_t = C_{\nu_t} \frac{k}{\omega}, C_{\nu_t} = 1,$$

and the near-wall ωcondition uses a wall coefficient $\omega_{\text{wall\_coeff}} = 85$ as defined in the solver implementation.

Near-wall behavior is enforced applying boundary values in the ghost cells adjacent to the no-slip wall. For the turbulent kinetic energy, the wall condition sets k to a near-zero value at the wall (consistent with a wall-resolved treatment where velocity fluctuations vanish at the boundary). For the specific dissipation rate, ω is prescribed using a wall formula of the form

$$\omega_w \propto \frac{\nu}{\Delta y_1^2},$$

where $\Delta y_1$is the wall-normal distance from the wall to the first cell center. This wall treatment is essential for stability and for obtaining physically consistent wall shear on wall-resolved meshes ($y^+ < 1$).

The ω-equation includes a production-like source and a dissipation term. Two equivalent production formulations were available in the implementation:

1. Production tied to P_k:

$$S_\omega = \gamma \left(\frac{\omega}{k}\right) P_k - \beta \omega^2$$

2. Production tied to mean strain-rate magnitude:

$$S_\omega = \gamma S^2 - \beta \omega^2$$

where S^2denotes the squared mean strain-rate magnitude (computed from local velocity gradients).

In this work the S^2-based formulation was used because it is numerically more robust for this solver and grid family. The $(\omega/k)P_k$form can become excessively stiff when k is very small (e.g., at early iterations or in near-wall cells), since the ratio ω/k can spike even with guard

values, leading to large local source terms and unstable updates. The S^2-based form removes the explicit ω/k factor, providing smoother source behavior during startup and on stretched near-wall meshes, while still coupling ω production to the resolved mean shear.

Target Reynolds number
To target Reynold number of 10,000, the flow is driven by a constant stream wise pressure gradient DPDX. For a fully developed internal flow, the Darcy friction factor relates to the pressure gradient through the following equation:

$$\frac{dp}{dx} = -f_D \frac{\rho \, U^2_{\text{bulk}}}{2D_h}.$$

An initial smooth wall estimate of f_D is 0.04 was used to estimate the forcing. Thus, DPDX = -0.057 is computed from the target Reynolds number and a friction factor estimate. The final friction factor is obtained from the final convergence value used for validation.

Turbulence Initialization
Turbulence quantities are initialized using turbulence intensity I and an integral length scale L. With $I = 0.05$, $L = 0.07D_h$ and $C_\mu = 0.09$,

$$k = \frac{3}{2}(U_{\text{bulk}} \, I)^2, \quad \omega = \frac{\sqrt{k}}{C_\mu^{1/4} \, L}.$$

The Turbulence intensity and length scale were assigned using standard empirical approximation for fully developed internal flows, while C_μ is the universally accepted empirical closure coefficient for a two-equation turbulence models. For $U_{\text{bulk}} = 0.75$ m/s, $D_h = 0.2$ m, and L = 0.014m, this yields k = $0.0021 m^2/s^2$, and $\omega = 6 \ s^{-1}$

Mesh Generation
To accurately capture the steep velocity gradients within the viscous sublayer without incurring massive computational costs, the baseline domain was discretized into a 10×30 rectangular grid. A geometric expansion ratio of 1.03 was applied in y-direction. This graded the mesh at the bottom of the wall without increasing mesh density on top symmetry boundary, achieving a y^+ value well suited for the wall bounded model

Time-Marching & Stability Parameters

Time marching is performed with an adaptive time step constrained by both advective and diffusive stability limits. The solver restricts the step size using a Courant number (CFL) and a diffusive Courant number, and additionally enforces a hard cap $\Delta t \leq \Delta t_{\max}$. In this study, CFL = 0.5, $\text{CFL}_{\text{diff}} = 0.5$, and $\Delta t_{\max} = 0.1$ were selected to maintain robust stability while converging efficiently. These values were chosen conservatively to prevent divergence in early iterations and to remain stable under near-wall grid stretching, where the smallest wall-normal spacing can impose a severe diffusion-driven time-step restriction.

3. Grid Dependency Study

A grid dependency study was conducted to evaluate how sensitive the predicted Darcy friction factor f_{wall} and near-wall resolution (y^+) are to mesh refinement. The three grids used in this study are shown in **Figure 1 (Coarse, Medium, Fine)**. All meshes were structured and used the same wall-normal geometric stretching ratio $r_y = 1.03$ to cluster cells near the no-slip wall.
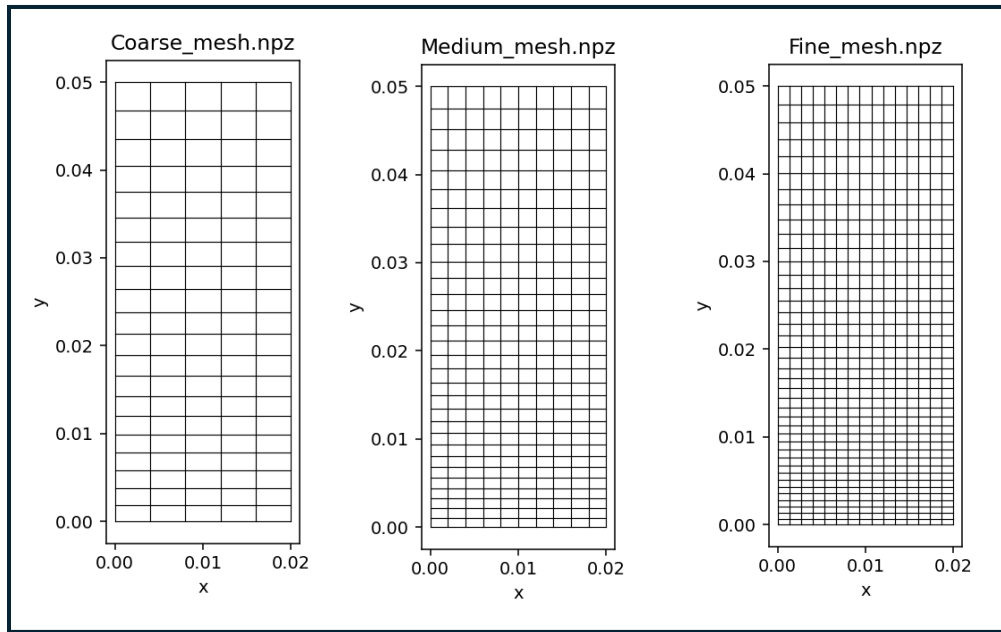

Figure 1 (Coarse, Medium, Fine)

Table 1 summarizes the friction factors obtained on each grid. Refinement from the Coarse (5×20) to Medium (10×30) mesh produced a small reduction in f_{wall} and improved agreement between the two friction-factor estimates (f_{dpdx} and f_{wall}). In contrast, the Fine (15×40) case did not follow the expected grid-convergence trend: while f_{dpdx} remained near 0.034, f_{wall} increased to 0.041. Because this change is inconsistent with monotonic grid convergence and

coincides with a much more restrictive time-marching setup (CFL = CFL_{diff} = 0.1, $\Delta t_{\max}$ = 0.01, 350,000 steps) and a different achieved Reynolds number ($Re \approx 9932$), the Fine-mesh result is treated as a stability/consistency outlier rather than evidence of a new grid-converged value. Therefore, the Medium (10×30) mesh is taken as the most reliable configuration for the primary results, balancing near-wall resolution with stable convergence and consistent friction-factor estimates.

Mesh	Cells (Nx × Ny)	[cfl, cfl_diff, dt_max, max_steps]	Re	f_{dpdx}	f_{wall}
Coarse	5 × 20	[0.5, 0.5, 0.1, 50000]	10755.5	0.035	0.034
Medium	10 × 30	[0.5, 0.5, 0.1, 100000]	10876.5	0.034	0.033
Fine	15 × 40	[0.1, 0.1, 0.01, 350000]	9932.15	0.034	0.041

Table 1

4. Results & Validation

Friction factor validation
The primary validation metric is the Darcy friction factor f_D. Using the Medium mesh, the simulation reached a steady fully developed state at a final Reynolds number of approximately $Re \approx 10{,}688$. At this Reynolds number, the smooth-wall reference friction factor from the Haaland/Moody correlation is $f_D \approx 0.0303$. The simulation produced a wall-based friction factor of $f_{wall} \approx 0.033$, corresponding to an overprediction of approximately 8.8%.

This bias is consistent with the numerical method used here: the 1st-order upwind convection scheme introduces numerical diffusion, which tends to increase effective dissipation near the wall and can shift the predicted wall shear upward.

Convergence history
Convergence to steady state was monitored using two independent friction-factor estimates: f_{wall}(from wall shear) and f_{dpdx}(from the imposed pressure gradient). Both quantities plateaued with iteration, indicating a steady solution. The final values remain close but not identical; the residual gap is attributed to discretization error and the different numerical evaluations used to compute each estimate.
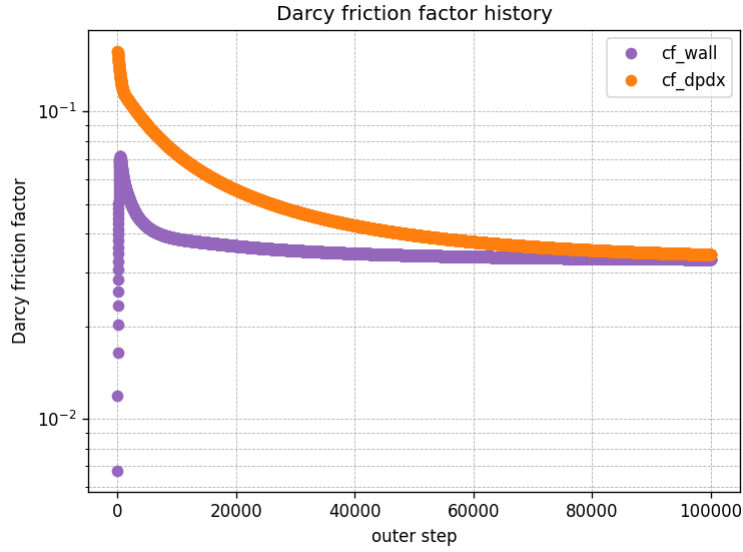
Figure 2: Friction factor convergence history (f_{wall} and f_{dpdx} vs iteration/time).

Flow-field and near-wall diagnostics

The converged solution shows the expected fully developed turbulent channel features. The mean streamwise velocity profile is noticeably flatter than the laminar parabolic profile, with the maximum velocity occurring at the symmetry boundary ($y = 0.05$ m). The transverse velocity remains negligible relative to the streamwise component ($|\,v\,| \ll |\,u\,|$), supporting a quasi-1D fully developed mean flow. The pressure field is included as a qualitative check that the imposed pressure-gradient forcing is being applied consistently and that no nonphysical pressure structure develops. Near-wall resolution is assessed using the y^+ diagnostic; the first-cell value on the Medium mesh is approximately $y^+ \approx 1.8$.
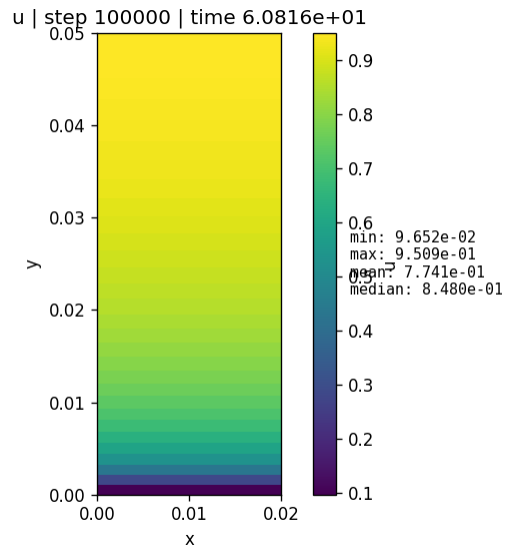
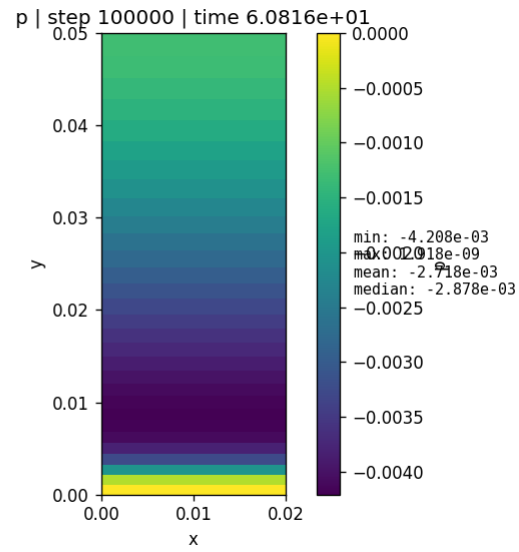**Figure 3: Contour plot of streamwise velocity, u(u.png).**

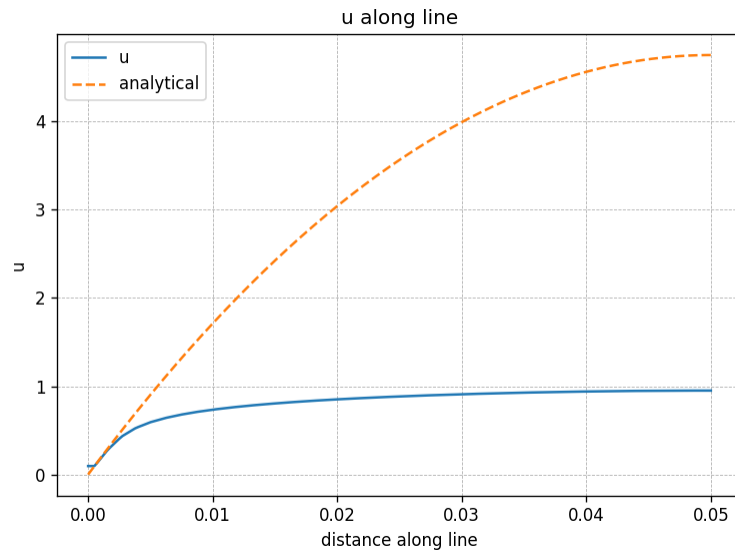**Figure 4: Contour plot of pressure field p(p.png).**

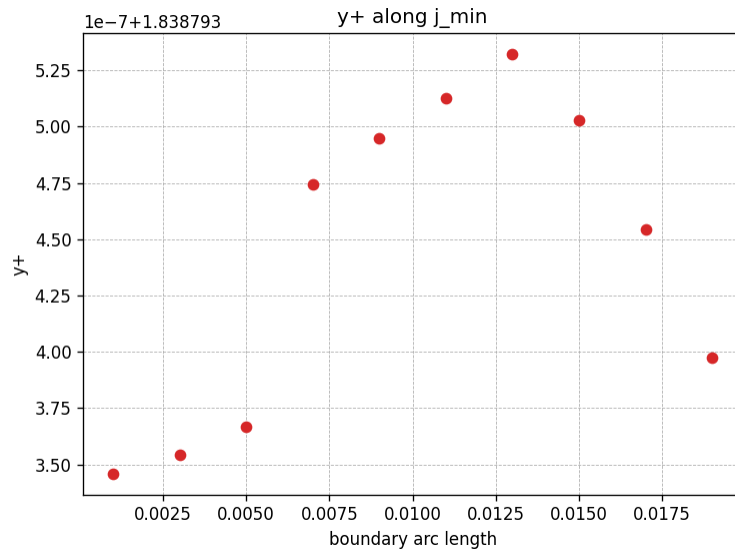**Figure 5: Centerline-normal velocity profile $u(y)$(u_line.png).**

Figure 6: y^+ distribution / first-cell y^+ diagnostic (yplus_v.png).
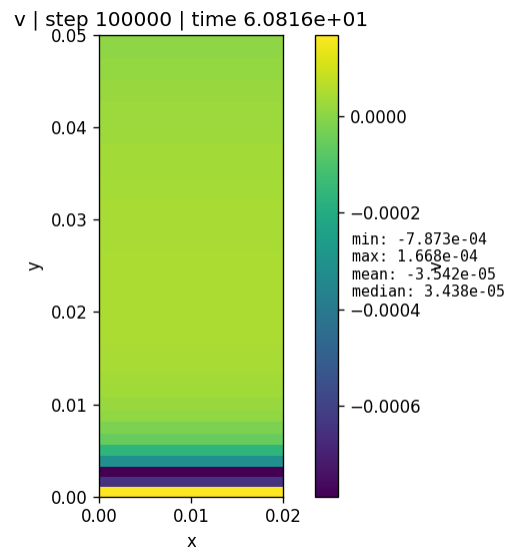

Figure 7: Contour plot of transverse velocity, v(v.png).

5. Discussion / Bonus Questions

Impact of initial conditions
Initializing with $u_{init} = U_{bulk}$ improves robustness and reduces startup transients. Starting from $u = 0$ yields near-zero shear and poorly conditioned turbulence initialization, which can produce extremely small k and unstable ω updates (even with guard values). A nonzero initial velocity field provides meaningful gradients from the first iterations, helping k–ω reach a physically reasonable state faster.

Turbulent viscosity in wall shear calculations
Wall shear stress should be evaluated using the molecular viscosity at the wall. In a wall-resolved formulation, turbulence is strongly damped at the boundary and ν_t should not directly contribute to the wall viscous stress. If ν_t is inadvertently included in the wall-shear evaluation (or remains artificially large in the first off-wall cell), τ_w and therefore f_{wall} can be biased high. In this report, the friction-factor bias is attributed primarily to numerical/near-wall sensitivity; a direct ν_t-leakage mechanism would require verifying how τ_w is computed in the implementation.

Why f_{wall} and f_{dpdx} do not match exactly
f_{dpdx} is inferred from the imposed forcing, while f_{wall} is computed from local near-wall gradients. During convergence they approach one another; a small steady offset can remain due to discretization error (notably 1st-order upwind), finite convergence tolerance, and the fact that the two metrics are computed through different numerical pathways. The key indicator of convergence is that both quantities reach stable plateaus.

Time step, CFL, and stability on stretched meshes
The time step controls both stability and the path to steady state. Tighter limits (lower CFL/ CFL_{diff} or smaller Δt_{max}) reduce iteration-to-iteration changes and prevent divergence, which becomes especially important as the wall-normal spacing is reduced by mesh stretching. Enforcing conservative CFL constraints keeps convective and diffusive updates stable in the smallest near-wall cells, at the cost of requiring more iterations to reach the final steady plateau.